Environ. Sci. Technol. **2008,** *42,* 5196–5201

Atmospheric Transport and Outflow of Polycyclic Aromatic Hydrocarbons from China

CHANG LANG,[†] SHU TAO,*[,†] WENXIN LIU,[†] YANXU ZHANG,[†] AND STACI SIMONICH[‡]

Laboratory for Earth Surface Processes, College of Environmental Sciences, Peking University, Beijing 100871, Department of Environmental and Molecular Toxicology and Department of Chemistry, Oregon State University, Corvallis, Oregon 97331

Received February 13, 2008. Revised manuscript received March 28, 2008. Accepted April 11, 2008.

A potential receptor influence function (PRIF) model, based on air mass forward trajectory calculations, was applied to simulate the atmospheric transport and outflow of polycyclic aromatic hydrocarbons (PAHs) emitted from China. With a 10 day atmospheric transport time, most neighboring countries and regions, as well as remote regions, were influenced by PAH emissions from China. Of the total annual PAH emission of 114 Gg, 92.7% remained within the boundary of mainland China. The geographic distribution of PRIFs within China was similar to the geographic distribution of the source regions, with high values in the North China Plain, Sichuan Basin, Shanxi, and Guizhou province. The Tarim basin and Sichuan basin had unfavorable meteorological conditions for PAH outflow. Of the PAH outflow from China (8092 tons or 7.1% of the total annual PAH emission), approximately 69.9% (5655 tons) reached no further than the offshore environment of mainland China and the South China Sea. Approximate 227, 71, 746, and 131 tons PAHs reached North Korea, South Korea, Russia-Mongolia region, and Japan, respectively, 2−4 days after the emission. Only 1.4 tons PAHs reached North America after more than 9 days. Interannual variation in the eastward PAH outflow was positively correlated to cold episodes of El Niño/Southern Oscillation. However, trans-Pacific atmospheric transport of PAHs from China was correlated to Pacific North America index (PNA) which is associated with the strength and position of westerly winds.

Introduction

Polycyclic aromatic hydrocarbons (PAHs) are recognized as a class of semivolatile organic compounds and are ubiquitous in ambient environment (*1*). Exposure to PAHs and PAH derivatives have been associated with cancers, especially lung cancer, which accounted for 1.3 million deaths worldwide in 2005 (*2*) (http://www.who.int/mediacentre/factsheets/fs297/en/index.html). Although historical data show that atmospheric PAH concentrations in the U.S. and Europe have declined gradually over the last century because of improved combustion technology and reductions in coal use (*3–5*), extensive and severe PAH pollution has been recently reported in developing countries with the largest populations in the world, including China, India, and Malaysia (*6–9*).

Based on global emission inventories, China had the greatest PAH emissions in the world (*10*). The total emission of 16 U.S. Environmental Protection Agency priority PAHs from China was 114 Gg/y in 2004, accounting for 22% of the worldwide PAH emissions (*10*). Indoor straw burning (34.6%), coke production (27.2%), indoor firewood burning (21.2%), and domestic coal combustion (6.8%) dominated the total PAH emissions from China (*11*). The PAH emission density from eastern China was significantly higher than western China. In addition, the PAH emissions from China have increased continuously since 1950 (*11*). Because of the intensive PAH emissions in China, high PAH concentrations have been measured in the environment (*6, 7*), leading to adverse impacts on human health (*12*). It was reported that the mean value of benzo[a]pyrene equivalent concentration in ambient air was as high as 2.54 ng/m^3 in Tianjin, China and over 40% of local human population was exposed to a concentration that exceeded the national standard of 10 ng/m^3, which is much higher than the national standard of developed countries (*5, 13*). Human exposure to high PAH concentrations through inhalation has also been confirmed in Shanghai, China (*14*).

In addition to local and regional impact, PAHs undergo long-range atmospheric transport to remote sites (*15, 16*). Measurements in the Northern Pacific Ocean, Arctic, and the west coast of North America suggest that atmospheric PAHs at these sites were related to biomass burning and coal combustion from continental sources (*16, 17*). By calculating potential receptor influence functions (PRIFs), PAH emissions from Guangdong, a southern province of China, were estimated to travel thousands of kilometers to Southeast Asia countries, the Koreas and the Pacific Ocean (*18*). In addition, elevated atmospheric PAH concentrations at Okinawa, Japan, Gosan, Korea, and remote sites on the west coast of the U.S. have been linked to PAH emission from China (*16, 19–21*).

Air mass trajectory modeling and statistics are commonly used to track the atmospheric transport of pollutants from source regions to receptor sites. A number of models, including potential source contribution functions, nonparametric regression models, and source region impact factors were established to identify the source regions of semivolatile organic chemicals based on air mass backward trajectory calculations (*19, 22, 23*). In our previous study, PRIF, which represents the probability of PAHs arriving at a receptor cell during a given transport time period, was developed based on air mass forward trajectory calculations and used to address the outflow of PAHs from Guangdong, China (*18*).

The objective of this research was to characterize the atmospheric dispersion of PAHs emitted from China, with an emphasis on the geographical distribution patterns within China and outflow to surrounding regions. The 16 PAH compounds modeled include naphthalene (NAP), acenaphthylene (ACY), acenaphthene (ACE), fluorene (FLO), phenanthrene (PHE), anthracene (ANT), fluoranthene (FLA), pyrene (PYR), benz[a]anthracene (BaA), and chrysene (CHR)) and particulate-phase (benzo(b)fluoranthene (BbF), benzo(k)-fluoranthene (BkF), benzo[a]pyrene (BaP), dibenz[a,h]anthracene (DahA), indeno[l,2,3-cd]pyrene (IcdP), and benzo[g,h,i]perylene (BghiP). Results for NAP, PHE, PYR, and BaP are shown as representative PAHs.

* Corresponding author phone and fax: 0086-10-62751938; e-mail: taos@urban.pku.edu.cn.
[†] Oregon State University.
[‡] Oregon State University.

10.1021/es800453n CCC: $40.75
Published on Web 06/06/2008

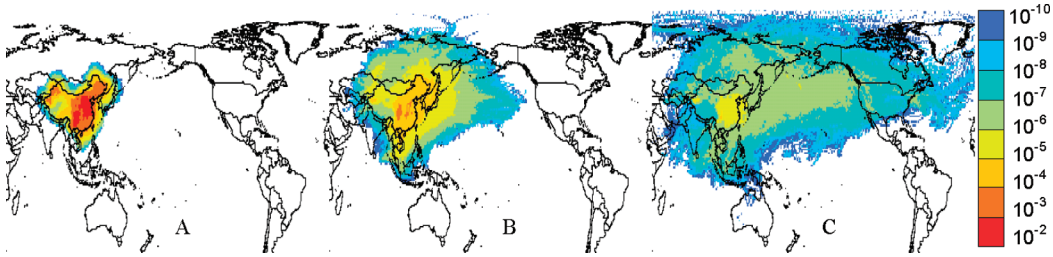

FIGURE 1. PRIF maps of PYR after a one (A), five (B), and 10 (C) day transport period as the annual mean of 2001.

Materials and Methods

Emission Inventory. In this study, a PAH emission inventory, with 1 × 1 km^2 resolution, was used to generate an inventory with 100 × 100 km^2 (1318 cells for the whole China) resolution ((*10*), see also Supporting Information Figure S1). A constant PAH emission rate was assumed because seasonal emission rates were not available.

Trajectory Calculation and Atmospheric Removal. Ten day forward air mass trajectories were calculated in 6 h intervals. The trajectories were calculated starting from the center of each of the 1318 emission cells using the National Oceanic and Atmospheric Administration's (NOAA) Hybrid Single-Particle Lagrangian Integrated Trajectory model (HYSPLIT) (*24*). NOAA-NCEP/NCAR's pressure level reanalysis data was used as the basis of the trajectory model. The vertical motion calculation method, top of model domain (the vertical limit of the internal meteorological grid), trajectory calculation initial times and start altitudes were the same as those used previously to study the outflow of PAHs from Guangdong, China (*18*). Pulsed PAH emissions, in 6 h intervals, were used as the starting points of each trajectory and the latitude-longitude coordinates of the calculated trajectory were recorded in 1 h intervals to derive 240 coordinate points for each trajectory. The atmospheric fate of PAHs, including gas-particle partitioning, photochemical degradation, and wet and dry deposition, were simulated along the trajectories and is described elsewhere (*18*) and in the Supporting Information. Using the PAH emission rate for each 100 × 100 km^2 cell and the estimated removal of PAHs from the atmosphere along the trajectory (due to advection, degradation, and deposition), the mass of PAHs along the 240 coordinate points of the trajectory was calculated.

Calculation of Potential Receptor Influence Function. A probability model using PRIF was used to depict the PAH dispersion pattern and outflow. The receptor cells were set at 1 × 1° horizontal resolution and 12 vertical levels (with the top of each level at 209, 495, 937, 1514, 2214, 3024, 4947, 6056, 7281, 8645, and 10155 m) following Harvard University's GEOS-CHEM model OH radical concentration data settings (http://www-as.harvard.edu/chemistry/trop/geos/geos_hi_res.html). The PRIF calculation has been previously described in ref *18* and in the Supporting Information. The PRIF represents the probability of PAHs arriving at a receptor cell during a given transport time period. For each emission pulse, the quantity of PAH arriving at a receptor cell, from all of the various trajectories, is summed over a given transport time period. The probability of PAHs reaching this receptor cell was calculated by dividing the quantity arriving at the receptor cell by the total quantity emitted from all of China. The results are presented as average probabilities over a defined emission period. All calculations were performed using Matlab and ArcGIS 9.0 was used for PRIF mapping and display.

Result and Discussion

Dispersion Pattern of PAHs Emitted from China. Ten day forward air mass trajectories were calculated for all of 2001 and 2002 at 6 h intervals. For model validation, the calculated one year time series of PYR PRIFs was compared with PAHs concentrations observed in Guangzhou, China and Gosan, Korea (*20, 25*). The trends were generally matched and the difference between the calculation and observation can be partially explained by the difference in the solution and the exclusion of the diffusion process in the model. The detailed results are presented in Supporting Information Figure S2. The annual mean PRIFs were used to illustrate the general atmospheric dispersion pattern of PAHs emitted from China. The elongated, eastward dispersion pattern in Figure 1 shows the annual mean PRIF maps after the 1st, 5th, and 10th day of the emission of PYR, a representative intermediate molecular weight PAH. Following one day of transport, PYR remained primarily within the boundary of mainland China, with limited outflow to neighboring countries and the geographic PAH distribution was not much different from the PAH emission inventory, suggesting a strong local source influence. PYR emissions from China reached East Asian and Southeast Asian countries, as well as the North Pacific Ocean, after a 5 day transport period. The PYR plume, carried by westerly winds, reached North America and Atlantic Ocean after a 10 day transport period. The trans-Pacific atmospheric transport of CO and PAHs from China has been discussed in the literature (*16, 21, 26*).

During atmospheric transport, the PAH concentrations decayed quickly due to degradation and wet and dry deposition. For example, the total PYR PRIFs decreased to 6.7 × 10^{-1}, 4.3 × 10^{-2}, and 3.1 × 10^{-3} after 1, 5, and 10 day transport periods, respectively. In addition to eastward transport, the transport of PAHs from China to the north, west, and south also occurred, but at much shorter distances. PRIFs in the 10^{-9} range were predicted to reach Australia, the Arctic, and middle-eastern countries within a 10 day transport period. The eastward long-range atmospheric transport of PAHs in the midlatitudes of the north hemisphere has been reported in the literature. Sehili suggested that PAHs emitted from Europe and Russia could be transported more than 10 000 km eastward (*27*). China's PAH emissions were believed to be responsible for the high atmospheric PAH concentrations measured in Gosan, a background site in Korea, from 2001 to 2004 (*20*). Of the various PAHs, the intermediate molecular weight PAHs (such as PYR) survived longer in the atmosphere than the others because of their slower degradation rate compared to lower molecular weight PAHs and lower deposition efficiency compared to higher molecular weight PAHs (*18*). For the same reasons, the intermediate molecular weight PAHs displayed higher vertical mobility than low and high molecular weight PAHs. The differences in the long-range transport potential of the PAHs are presented in detail in Supporting Information Figure S3.

To quantify the PAH transport in both direction and distance, the gravity center of the PRIFs was calculated as follows:

$$C(i,j) = (\Sigma \mathrm{PRIF}_{i,j} \times i / \Sigma \mathrm{PRIF}_{i,j}\ ' \Sigma \mathrm{PRIF}_{i,j} \times j / \Sigma \mathrm{PRIF}_{i,j}) \quad (1)$$

where $C(i, j)$ are coordinates of the gravity center and $\mathrm{PRIF}_{i,j}$ is PRIF value of the receptor cell (i, j). The gravity center pathways during a 10 days transport period illustrates the general trends of PAH transport from China (Supporting

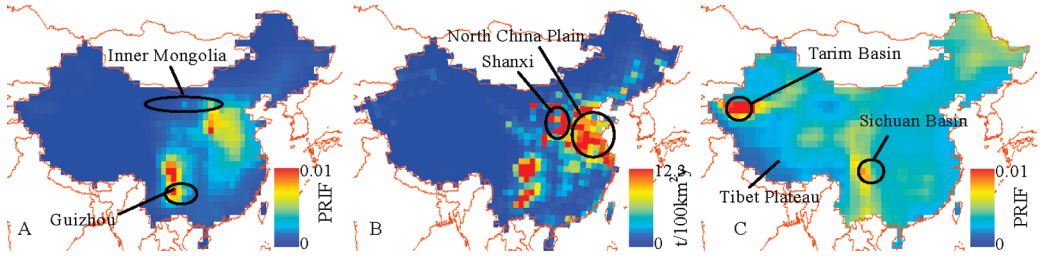

FIGURE 2. Comparison of the PYR geographic distribution pattern of the annual mean PRIF based on a 10 day transport period (A), emission inventory of PYR (B) and annual mean PYR PRIF map derived based on a uniform emission density throughout China (C).

Information Figure S4). Significant differences in long-range transport potential (the speed of the gravity center movement), in direction of the transport as well as the extent of dispersion (interquartile range of the PRIFs), were observed among the four PAHs. The two more volatile PAHs (NAP and PHE) traveled quickly in a northeasterly direction across 15 degrees of latitude during 10 days, whereas PYR and BaP traveled in an easterly direction at a relatively slow pace along the meridional direction. This difference in transport direction is consistent with global fractionation theory which suggests that more volatile compounds have a greater potential to be transported to and deposited in higher latitudes than less volatile compounds which tend to stay closer to source regions (*28, 29*). In addition, the more volatile PAHs dispersed over larger geographic areas than the less volatile PAHs during atmospheric transport (Supporting Information Figure S4). The zonal interquartile NAP range reached 56 degrees longitude in a 10 day transport period compared to 50, 42, and 24 degrees for PHE, PYR, and BaP, respectively.

Geographic Distribution of PAHs within Mainland China. Because the majority of emitted PAHs remained within China, the geographic distribution pattern of PAHs within mainland China was of interest for exposure risk assessment. In Figure 2, the annual mean PRIF (10 day transport period) (A) and emission density (B) of PYR are mapped. Similar to the emission inventory, the PRIF shows a distribution pattern with higher values in eastern China where the population density and energy consumption rate were much higher than the rest of China. Higher PRIFs values ($>10^{-3}$) were predicted in Shanxi, Sichuan, Guizhou, and the Northern China Plain, whereas lower PRIFs ($<10^{-4}$) were predicted in Inner Mongolia and the western Chinese provinces. The PYR PRIF map was consistent with the map of Aerosol Optical Thickness derived from MODIS images (Supporting Information Figure S5).

The PYR PRIF map (Figure 2A) shows the combined effects of both emissions and meteorological conditions on the PYR distribution, whereas Figure 2C shows the influence of meteorological conditions only, assuming a uniform PYR emission density throughout China. To prevent underestimation of PYR PRIFs due to missing emission data for countries immediately surrounding mainland China, a uniform emission density was also assumed for these geographic areas. The areas with relatively high PRIFs included the Sichuan Basin and the Tarim Basin which are sheltered by the Tibetan Plateau, creating unfavorable conditions for dispersion. During the cold season, the "warm low" influenced the entire Tarim Basin region and atmospheric transport was limited locally to the lower troposphere (*30*). The accumulation of aerosol in the Sichuan Basin has also been observed by model simulation (*31*).

Using PYR as an example, the spatial distribution of the annual mean transport fluxes in China and the surrounding areas, that result from the geographic distribution of both emissions and meteorological conditions, are illustrated in Supporting Information Figure S6. A clockwise horizontal transport pattern, centered in the North China Plain, can be seen at 0−1 km altitude layer. On an annual average basis, the Sichuan Basin and the Yunnan-Guizhou highland had the greatest PYR fluxes in a northwesterly direction in the boundary layer (Supporting Information Figure S6A). The PYR flux shifted in a northeasterly (Supporting Information Figure S6B) and easterly direction in the free troposphere (Supporting Information Figure S6C). Because of the specific meteorological (large scale convergence) and topographical (negative landform and orographic forcing) conditions, as well as the extremely high PAH emission rates, the most intensive uplifting occurred in the Sichuan basin (Supporting Information Figure S6D and refs *26 and 32)*.

In the boundary layer of eastern China, PAH transport in the northeasterly and easterly directions occurred at latitudes north of 35° N, whereas transport in the southwesterly and southerly directions occurred at latitudes south of 35° N. In a survey conducted in the winter of 2005, Liu et al. found that PAHs emitted from the North China Plain were transported either southward along the coast of China or eastward to Korea, Japan, and the Pacific Ocean (*6*). This boundary layer transport, which resulted in PAH outflow from China, was attributed to transport behind cold fronts (*26, 33*). In the mid troposphere (1−5 km), eastward movement dominated the transport. However, the fluxes were 1 order of magnitude less than the boundary layer transport fluxes, with the strongest easterly transport occurring around 30° N. In the upper troposphere (5−10 km), the horizontal PYR transport flux was almost 3 orders of magnitude less than those in the boundary layer because of the extremely low concentrations even though the wind speed was the fastest. Easterly transport in the upper troposphere was limited to 30° N, whereas westerly transport was also predicted in the upper troposphere, the fluxes were much smaller.

Outflow of PAHs from China. Even though 92.7% of PAHs emitted in China remained within continental China, a significant amount of PAHs were predicted to undergo atmospheric transport and outflow to other regions of the world. For quantitative illustration, the outflow of PAHs from China to a given region or country was calculated as the total PAH flux from China that was degraded in or deposited to the region or country. The outflow to a country was calculated based on the PRIFs and the annual Chinese PAH emission rate which was estimated to be 113 859 ton/year (*10*). Among the 8092 tons of PAHs (7.1% of the total emission) that were transported out of mainland China, a large portion (69.9%) reached no further than the offshore environment (4664 tons) and the South China Sea (991 tons). The remaining 2437 tons were transported to Russia and Mongolia (746 tons), North Korea (227 tons), South Korea (71 tons), Japan (131 tons), Middle Asia (129 tons), South Asia (28 tons), the Pacific Ocean (742 tons), and North America (1.4 tons), respectively (Supporting Information Table S2). The PAH outflow from China to these regions or countries was a relatively small percentage of the PAH emissions within these regions or countries (approximately 1% of Middle Asia and Southeast Asia countries, 0.03% of South Asia, and 2% of Japan's emission) except for North Korea (11.5%), South Korea (8.5%), and Russia and Mongolia (8.0%).

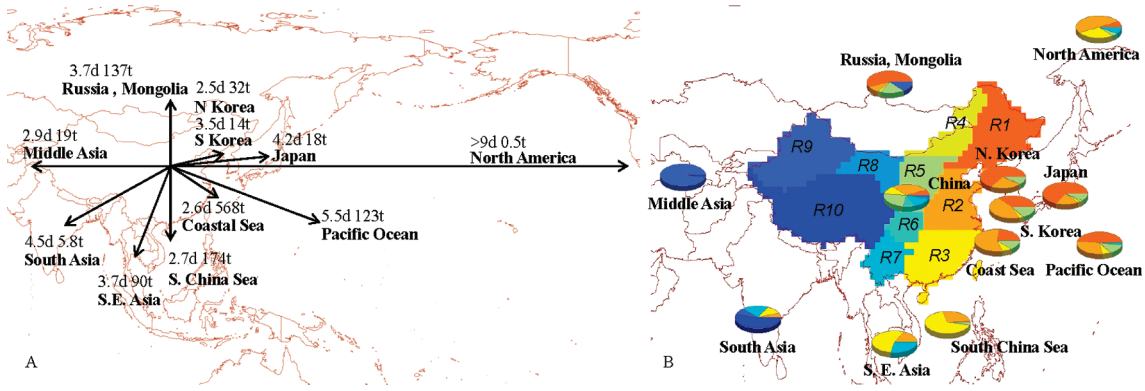

FIGURE 3. Annual outflows and mean transit times (MTT) of PYR from China to other countries/regions (A) and the relative contributions (pie slices) of various source regions within mainland China to the outflow (B). Regions 1−10 are Northeast China, North China Plain, and Jianghuai Plain, Southeast China, Daxing Mountain region, Loess plateau, Sichuan basin, Yunnan-Guizhou Highland, Gobi desert, Xinjiang province, and Tibet-Qinghai plateau, respectively.

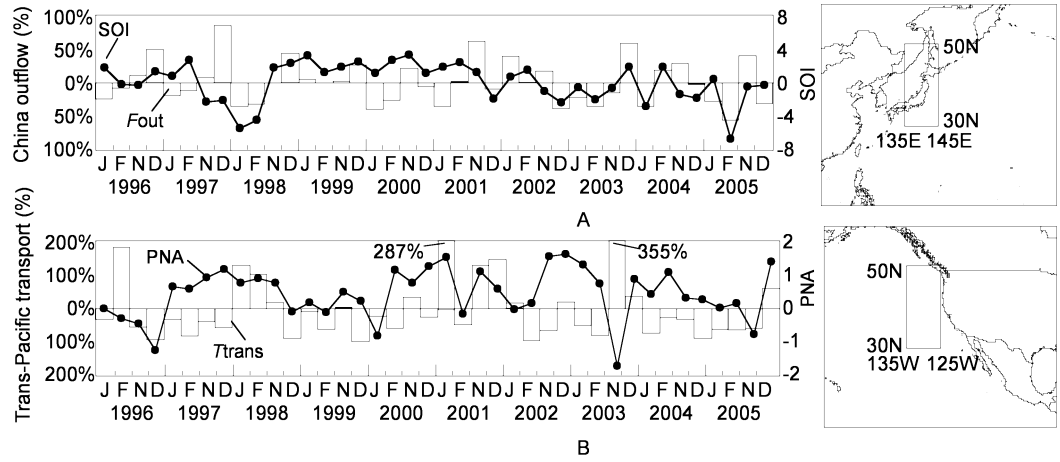

FIGURE 4. Interannual variation of PYR outflow from China in winter (A, *F*out) and trans-Pacific transport (B, *T*trans). The results are presented as the standardized monthly PYR PRIF anomalies for the two rectangular receptor site areas (30−50° N, 135−145° E and 30−50° N, 125−135° W). *F*out and *T*trans are compared with South Oscillation Index (SOI) and Pacific North America indices (PNA).

In addition to the PAH quantities, the mean transit times (MTT), defined as the PRIF-weighted mean time required for PAHs to reach a region or country, was calculated:

$$\mathrm{MTT(R)} = (\Sigma \mathrm{PRIF}_T\mathrm{(R)} \times \mathrm{day}/\Sigma \mathrm{PRIF}_T\mathrm{(R)}) \qquad (2)$$

where MTT(R) is mean transit time from China to region *R* and PRIF_T(R) represents the T^{th} transport day PRIF in region R. Figure 3A illustrates the calculated MTT for PYR along with its annual outflow quantities. The corresponding NAP, PHE and BaP results are presented in Supporting Information Tabel S2. In general, it took 2∼4 days for PAHs to travel from China to neighboring regions. For example, the MTT was 1.9 days for NAP to reach the South China Sea, 2.6 days for PYR to reach the offshore environment, and 3.5 days for PHE to reach Japan. The calculated MTT of PYR to North America was more than 9 days. This is similar to the calculated CO transport times from eastern China to western North America in spring (8 days in the upper troposphere and 14 days in the lower tropophere) (*34*).

As expected, both the outflow and MTT were individual PAH compound dependent. Of the four representative PAHs, BaP, and other high molecular weight PAHs, are predominately associated with air borne particles (*35*) and are primarily transported to other regions in the lower atmosphere, whereas low molecular weight PAHs are more often transported in the free-troposphere. Consequently, BaP had the longest MTT from China to Russia-Mongolia, South East Asia, South Korea, Japan, Pacific Ocean, and North America, but the shortest MTT to regions which were located closer to the source region.

Depending on differences in emission density, location, and meteorological conditions, the contributions of various source regions within China to the PAH outflow were significantly different. To demonstrate this difference, China was divided into ten source regions based on PAH emission density, climate, and land formation (Figure 3B). PRIFs were calculated separately for individual PAH emission region and Figure 3B shows the relative contributions of the ten regions to the PYR outflow to various receiving countries and regions. It appears that three source regions, including northeast China, the North China Plain, and the Loess plateau, contribute 88% of the easterly PYR outflow. The northwesterly wind (which occurs most frequently during the winter and spring months) transported PAHs emitted in the boundary layer of northeastern China off continent in the lower troposphere to Korea, Japan and the Pacific Ocean. As a result, 98 and 94% of PYR transported from China to North Korea and Japan, respectively, were from northeastern China. Southerly winds (which occur more frquently in summer) transported PAHs from northeast China in a northwesterly direction in the lower troposphere, resulting in 54% of the annual PAH outflow to Mongolia-Russia. Of the PAH outflow that reached South Korea and areas offshore of China, 43 and 56% were from the North China Plain and 23 and 38% were from northeast China, respectively. Southeast China was a major contributor to the PAH outflow reaching the South China Sea (68%) and Southeast Asia (54%). Most of the PYR emissions (81%) that were uplifted and carried away by westerly winds to North America were from the North China Plain and Southeast China. The maximum eastward

outflow of PAHs from China occurred around 40° N, except for high molecular weight PAHs such as BaP, which were primarily from southern China (Supporting Information Figure S7).

Although Sichuan Basin is one of the regions in China with an extremely high PAH emission density (Figure 2B), it did not contribute a large share to the total PAH outflow, except for a relatively small fraction to Southeast Asia (28%). As discussed previously, the local meterological conditions and topography prevented the outflow of PAHs in the lower atmosphere which results in severe local contamination in Sichuan (Figure 2A). Tibet contributed a large fraction (53%) of the total PAH outflow to South Asia and the Indian Ocean with most of which reached no farther than Bhutan and Nepal. The westerly PAH outflow was significantly less than the easterly PAH outflow due to meteorological conditions in China, as well as the difference in PAH emission density between western and eastern China; 96.6% of the westerly PAH outflow to middle and west Asian countries was from Xinjiang and only reached Kazakhstan, Kyrgyzstan, and Tajikistan, which are immediately adjacent to Xinjiang.

Both vertical forcing and zonal winds are required for trans-Pacific atmospheric transport of pollutants (*26, 34, 36, 37*). In order to undergo trans-Pacific atmospheric transport, PAHs must be uplifted into the troposphere where they are carried by strong westerly winds. Both midlatitude cyclones and convection can swiftly uplift pollutants and the warm conveyor belt (associated with midlatitude cyclones) dominate the uplifting in midlatitude Asia (*36, 37*). As a result, approximately 80% of the predicted trans-Pacific atmospheric transport of PAHs occurred during 14 days in 2001 when the meterological conditions were favorable for the transport. For example, during the period of January 20−23, 2001, severe cold surges hit China, resulting in strong frontal uplifting and trans-Pacific atmospheric transport (*18*).

Interannual Variation in Outflow. Monthly mean PRIFs of the representative PAHs were calculated from 1996 to 2005 to understand the interannual variation in PAH outflow and the possible relationship between the dynamic variation in the outflow and climate. The interannual variation outflow of PAHs from China and trans-Pacific atmospheric transport was investigated by calculating PYR PRIFs for two receptor site areas: (A) an area between 30−50° N and 135−145° E near Northeast China for PAH outflow, and (B) an area between 30−50° N and 125−135° W near the west coast of the United States for PAH trans-Pacific atmospheric transport, respectively. The strongest outflow was found in the winter from November to February each year except 1999 and 2004. Therefore, only the results of November, December, January, and February, denoted as *F*out and *T*trans, are present in Figure 4.

As discussed previously, transport in the boundary layer was primarily responsible for transport of PAHs offshore from mainland China (*F*out), whereas the transport in the free troposphere was primarily responsible for PAH trans-Pacific atmospheric transport (*T*trans). As a result, the coefficients of variance for the annual mean *F*out and *T*trans was 7 and 50%, respectively, indicating that trans-Pacific atmospheric transport was much more sensitive to changes in meteorological conditions.

The interannual variation of *F*out is compared with the Southern Oscillation Index (SOI, http://www.cpc.noaa.gov/data/indices/soi) as an indicator of El Niño/Southern Oscillation in Figure 4A. A statistically significant ($p = 0.034$; Spearman correlation coefficient = 0.335) positive correlation existed between PYR *F*out and SOI. It also appears that the winter PYR outflow from China was strongly influenced by cold episodes (positive SOI) due to the association between the high frequency of cold episodes and intense boundary outflow behind the front (*26*).

No significant correlations were found between SOI and PYR *T*trans ($p = 0.65$), but a significantly positive correlation ($p = 0.023$; Spearman correlation coefficient = 0.359) existed between PYR *T*rans and the Pacific North America index (PNA, http://www.cpc.ncep.noaa.gov/products/precip/CWlink/pna/pna.shtml), with November 2003 being the only exception (Figure 4B). A positive PNA has been associated with enhanced East Asian jet streamflow and dust storms (*38*). It has also been reported that an enhanced Aleutian Low and Pacific high are favorable for the transport of atmospheric pollutants from East Asia to North America and the pressure level system was associated with PNA (*36*). It should be noted that other factors, including the location of the warm coveyor belt (which is difficult to quantify), are also important factors influncing trans-Pacific atmospheric transport (*37*).

Acknowledgments

The funding of this study was provided by the National Science Foundation of China (Grant 140710019001 and 40730737) and National Basic Research Program (2007CB407303).

Supporting Information Available

Detailed methodology and more results. This material is available free of charge via the Internet at http://pubs.acs.org.

Literature Cited

(1) *Environmental Health Criteria 202: Selected Non-Heterocyclic Polycyclic Aromatic Hydrocarbons*, World Health Organization: Geneva. 1998.
(2) Perera, F. P. Environment and cancer. Who are susceptible? *Science* **1997**, *278*, 1068–1073.
(3) Jones, K. C.; Sanders, G.; Wild, S. R.; Burnett, V.; Johnston, A. E. Evidence for a decline of PCBs and PAHs in rural vegetation and air in the United Kingdom. *Nature* **1992**, *356*, 137–140.
(4) Harrison, R. M.; Grieken, R. E. *Atmospheric Particles IUPAC Series on Analytical and Physical Chemistry of Environmental System; v. 5*; John Wiley & Sons Ltd: England, 1998.
(5) WHO. *Air Quality Guidelines for Europe, 2nd edition-Copenhagen. WHO Regional Office for Europe, Publication No. 91*; World Health Organization: Geneva, 2000.
(6) Liu, S. Z.; Tao, S.; Liu, W. X.; Liu, Y. N.; Dou, H.; Zhao, J. Y.; Wang, L. G.; Wang, J. F.; Tian, Z. F.; Gao, Y. Atmospheric polycyclic aromatic hydrocarbons in North China a wintertime study. *Environ. Sci. Technol.* **2007**, *41*, 8256–8261.
(7) Wang, G. H.; Kawamura, K.; Lee, S.; Ho, K. F.; Cao, J. J. Molecular, seasonal, and spatial distributions of organic aerosols from fourteen Chinese cities. *Environ. Sci. Technol.* **2006**, *40*, 4619–4625.
(8) Sharma, H.; Jain, V. K.; Khan, Z. H. Characterization and source identification of polycyclic aromatic hydrocarbons PAHs) in the urban environment of Delhi. *Chemosphere* **2007**, *66*, 302–310.
(9) Bin Abas, M. R.; Rahman, N. A.; Omar, N.Y.M.J.; Maah, M. J.; Abu Samah, A.; Oros, D. R.; Otto, A.; Simoneit, B. R. T. Organic composition of aerosol particulate matter during a haze episode in Kuala Lumpur, Malaysia. *Atmos. Environ.* **2004**, *38*, 4223–4241.
(10) Zhang Y. X., personal communication. ,
(11) Zhang, Y. X.; Dou, H.; Chang, B.; Wei, Z. C.; Qiu, W. X.; LiuS. Z.; Liu, W. X.; Tao, S., Emission of polycyclic aromatic hydrocarbons (PAHs) from indoor straw burning and emission inventory updating in China., *Annu. NY Acad. Sci.* in press.
(12) Zhang, J. F.; Smith, K. R. Household air pollution from coal and biomass fuels in China: measurements, health impacts, and interventions. *Environ. Health Perspect.* **2007**, *115*, 848–855.
(13) Tao, S.; Li, X. R.; Yang, Y.; Coveney, R. M.; Lu, X. X.; Chen, H. T.; Shen, W. R. Dispersion modeling of polycyclic aromatic hydrocarbons from combustion of biomass and fossil fuels and production of coke in Tianjin, China. *Environ. Sci. Technol.* **2006**, *40*, 4586–4591.
(14) Cheng, J. P.; Yuan, T.; Wu, Q.; Zhao, W. C.; Xie, H. Y.; Ma, Y. G.; Ma, J.; Wang, W. H. PM10-bound polycyclic aromatic hydrocarbons (PAHs) and cancer risk estimation in the atmosphere surrounding an industrial area of Shanghai, China. *Water, Air, Soil Pollut.* **2007**, *183*, 437–446.

(15) Halsall, C. J.; Barrie, L. A.; Fellin, P.; Muir, D. C. G.; Billeck, B. N.; Lockhart, L.; Rovinsky, F. Y. A.; Kononov, E. Y. A.; Pastukhov, B. Spatial and temporal variations of polycyclic aromatic hydrocarbons in the Arctic atmosphere. *Environ. Sci. Technol.* **1997**, *31*, 3593–3599.
(16) Primbs, T.; Piekarz, A.; Wilson, G.; Schmedding, D.; Higginbotham, C.; Field, J.; Simonich, S. Influence of Asian and western U.S. urban areas and fires on the atmospheric transport of PAHs, PCBs, and FTOHs in the western U.S. *Environ. Sci. Technol.* in press.
(17) Ding, X.; Wang, X. M.; Xie, Z. Q.; Xiang, C. H.; Mai, B. X.; Sun, L. G.; Zheng, M.; Sheng, G. Y.; Fu, J. M.; Poschl, U. Atmospheric polycyclic aromatic hydrocarbons observed over the North Pacific Ocean and the Arctic area: Spatial distribution and source identification. *Atmos. Environ.* **2007**, *41*, 2061–2072.
(18) Lang, C.; Tao, S.; Zhang, G.; Fu, J. M.; Simonich, S. L. Outflow of polycyclic aromatic hydrocarbons from Guangdong, southern China. *Environ. Sci. Technol.* **2007**, *41*, 8370–8375.
(19) Primbs, T.; Simonich, S. L.; Schmedding, D.; Wilson, G.; Jaffe, D.; Takami, A.; Kato, S.; Hatakeyama, S.; Kajii, Y. Atmospheric outflow of anthropogenic semi-volatile organic compounds from East Asia in spring 2004. *Environ. Sci. Technol.* **2007**, *41*, 3551–3558.
(20) Lee, J. Y.; Kim, Y. P.; Kang, C. H.; Ghim, Y. S.; Kaneyasu, N. Temporal trend and long-range transport of particulate polycyclic aromatic hydrocarbons at Gosan in northeast Asia between 2001 and 2004. *J. Geophys. Res., [Atmos.]* **2006**, *111*, D11303.
(21) Killin, R. K.; Simonich, S. L.; Jaffe, D. A.; DeForest, C. L.; Wilson, G. R. Transpacific and regional atmospheric transport of anthropogenic semivolatile organic compounds to Cheeka Peak Observatory during the spring of 2002. *J. Geophys. Res. [Atmos.]* **2004**, *109*, D23S15.
(22) Hoh, E.; Hites, R. A. Sources of toxaphene and other organochlorine pesticides in North America as determined by air measurements and potential source contribution function analyses. *Environ. Sci. Technol.* **2004**, *38*, 4187–4194.
(23) James, R. R.; Hites, R. A. Atmospheric transport of toxaphene from the Southern United States to the Great Lakes region. *Environ. Sci. Technol.* **2002**, *36*, 3474–3481.
(24) Draxler, R. R.; Rolph, G. D. *HYSPLIT (HYbrid Single-Particle Lagrangian Integrated Trajectory*; NOAA Air Resources Laboratory: Silver Spring MD, 2003; http://www.arl.noaa.gov/ready/hysplit4.html.
(25) Li, J.; Zhang, G.; Li, X. D.; Qi, S. H.; Liu, G. Q.; Peng, X. Z. Source seasonality of polycyclic aromatic hydrocarbons (PAHs) in a subtropical city, Guangzhou, South China. *Sci. Total Environ.* **2006**, *355*, 145–155.
(26) Liu, H. Y.; Jacob, D. J.; Bey, I.; Yantosca, R. M.; Duncan, B. N. Transport pathways for Asian pollution over the Pacific: Interannual and seasonal variations. *J. Geophys. Res., [Atmos.]* **2003**, *108*, D20–8786.
(27) Sehili, A. M.; Lammel, G. Global fate and distribution of polycyclic aromatic hydrocarbons emitted from Europe and Russia. *Atmos. Environ.* **2007**, *41*, 8301–8315.
(28) Wania, F.; Mackay, D. Tracking the distribution of persistent organic pollutants. *Environ. Sci. Technol.* **1996**, *30*, A390–A396.
(29) Simonich, S. L.; Hites, R. A. Global distribution of persistent organochlorine compounds. *Science* **1995**, *269*, 1851–1854.
(30) Xuan, J.; Sokolik, I. N.; Hao, J. F.; Guo, F. H.; Mao, H. Q.; Yang, G. M. Identification and characterization of source of atmospheric mineral dust in East Asia. *Atmos. Environ.* **2004**, *38*, 6239–6252.
(31) Huang, Y.; Dickinson, R. E.; Chameides, W. L. Impact of aerosol indirect effect on surface temperature over East Asia. *Proc. Natl. Acad. Sci. U. S. A.* **2006**, *103*, 4371−4376.
(32) Bey, I.; Jacob, D. J.; Logan, J. A. YantoscaR.M. Asian chemical outflow to the Pacific in spring: Origins, pathways, and budgets. *J. Geophys. Res. [Atmos.]* **2001**, *106*, 097−23–114.
(33) Carmichael, G. R.; Tang, Y.; Kurata, G.; Uno, I.; Streets, D.; Woo, J. H.; Huang, H.; Yienger, J.; Lefer, B.; Shetter, R. Regional-scale chemical transport modeling in support of the analysis of observations obtained during the TRACE-P experiment. *J. Geophys. Res., [Atmos.]* **2003**, *108*, NO.D21–8823.
(34) Holzer, M.; Mckendry, I. G.; Jaffe, D. A. Springtime trans-Pacific atmospheric transport from east Asia: A transit-time probability density function approach. *J. Geophys. Res., [Atmos.]* **2003**, *108*, D22 4708.
(35) Su, Y. S.; Lei, Y. D.; Wania, F.; Shoeib, M.; Harner, T. Regressing gas/particle partitioning data for polycyclic aromatic hydrocarbons. *Environ. Sci. Technol.* **2006**, *40*, 3558–3564.
(36) Liang, Q.; Jaegle, L.; Wallance, J. M. Meteorolical indices for Asian outflow and transpacific transport on daily to interannual timescales. *J. Geophys. Res., [Atmos.]* **2003**, *110*, D18308.
(37) Stohl, A. A 1-year Lagrangian "climatology" of airstreams in the northern hemisphere troposphere and lowermost stratosphere. *J. Geophys. Res., [Atmos.]* **2001**, *106*, 7263–7279.
(38) Gong, D. Y.; Mao, R.; Shi, P. J.; Fan, Y. D. Correlation between east Asian dust storm frequency and PNA. *Geophys. Res. Lett.* **2007**, *34*, L14710.

ES800453N